THE ASTROPHYSICAL JOURNAL, 279:74–85, 1984 April 1

ALTERNATING-SIDE EJECTION IN EXTRAGALACTIC RADIO SOURCES

L. RUDNICK AND B. K. EDGAR
University of Minnesota
Received 1983 January 14; accepted 1983 September 2

ABSTRACT

Analyses of radio galaxy and QSO maps provide evidence for a *preferential avoidance* of structures at the same nuclear distance on the two sides of a source. We show that such an effect is most likely due to ejections from the nucleus occurring on only one side at a time. Under this model, strict constraints are placed on the ejection velocities, the amount of "cold" material carried along with the relativistic electrons, and the power supply to jets and hot spots. We discuss some theoretical difficulties raised by this model, and refer to current ideas about forming one-sided sources. We demonstrate the lack of a clear signature in other observational tests, and suggest future work. Throughout the paper, we call attention to the very limited nature in which extragalactic radio sources are symmetric.

Subject headings: galaxies: jets — particle acceleration — quasars — radio sources: galaxies

I. INTRODUCTION

"Classical double" radio sources earn their name from the symmetric appearance of their extended lobes (Miley 1980; Ekers 1982). One-sided sources—e.g., Miley's (1971) extended D2 objects, or VLBI jets (Kellermann and Pauliny-Toth 1981)—are the exception, not the rule. However, increasingly high resolution studies of radio galaxies and QSOs have shown substantial differences in component size, shape, and strength (e.g., Neff and Rudnick 1980; Macklin 1981) between the two lobes.

Figure 1 illustrates this point. We have randomly selected a group of radio sources from those mapped by Riley and Pooley (1975), and have cut them in half, with each half arbitrarily placed in one column. Matching up the respective source halves will be a difficult exercise for most readers, especially if secondary clues such as beam shape and contour level are ignored. The point is that radio lobes are almost as similar *between sources* as they are between the two sides of the same source. Continuing discoveries of one-sided extended jets (see review by Bridle 1982) have intensified the interest in radio source asymmetries.

Why are the two sides different? Among the ideas proposed are time delay effects (Ryle and Longair 1967), ambient medium fluctuations (e.g., Miley 1980), relativistic beaming (Shklovsky 1977), anisotropic electron pitch-angle distributions (van Groningen, Miley, and Norman 1980), and transient phenomena (Christiansen, Pacholcyzk, and Scott 1982). In this paper we present the case for a specific pattern to the asymmetries between sides of an individual source, namely that *where an emission peak occurs on one side of a source, no peak will be found at the corresponding distance on the other side of the nucleus* (Rudnick 1982). We examine the possible explanations for this "avoidance" behavior, and discuss the possibility that it is due to alternating-side ejections from the nuclear source. This possibility has been mentioned, and dismissed, by Birkinshaw, Laing, and Peacock (1981), van Groningen, Miley, and Norman (1980), Willis, Wilson, and Strom (1978), Saikia and Wiita (1982), and Rees (1982). Macklin (1981) mentions it as a possible explanation for his asymmetry statistics, and Robson (1981) proposes it to explain the structure of 3C 133. Shklovsky (1982) also suggests, as we do, that one-sided jets may be due to single-sided energy sources, and he examines the consequences of momentum conservation in the nucleus.

The organization of the paper is as follows: In § II we examine the specific patterns of source asymmetries in a few different ways, and show why many common dynamical arguments cannot explain the data. In § III we explore a few mechanisms which can produce the observed avoidance and comment on their strengths and problems. In § IV we outline the implications for the inertia of the ejected material, the properties of the surrounding medium, the need for localized particle acceleration, and the nature of the nuclear engine, assuming that the nucleus does alternate its ejection direction. In § V we mention the problems which one-sided ejection models face due to observations of very symmetric sources and relativistic beaming; we summarize our understanding to date, and suggest work for the future.

II. OBSERVATIONAL EVIDENCE AND EMPIRICAL MODELS

a) Visual Impressions

The first suggestive evidence of what we propose to call the "specific avoidance" effect came from visual examination of contour maps. A large number of high-resolution maps were rotated 180° around their cores (for rotation [S] symmetric sources) or reflected about their symmetry axis (for mirror [C] symmetric sources) and then overlaid on their respective originals. It was apparent that the high surface brightness regions from one side "avoid" those from the other side, for most sources.

Figure 2 (Plates 1 and 2) illustrates this effect. We have selected some of the best examples of avoidance, to clarify its nature. Sources dominated by only a single hot spot on each side almost always show avoidance, but the sources with more complicated structures are critical to some of the arguments discussed below.

Examination of Figure 2 also raises the problems associated with making a quantitative test of the avoidance effect.

PLATE 1

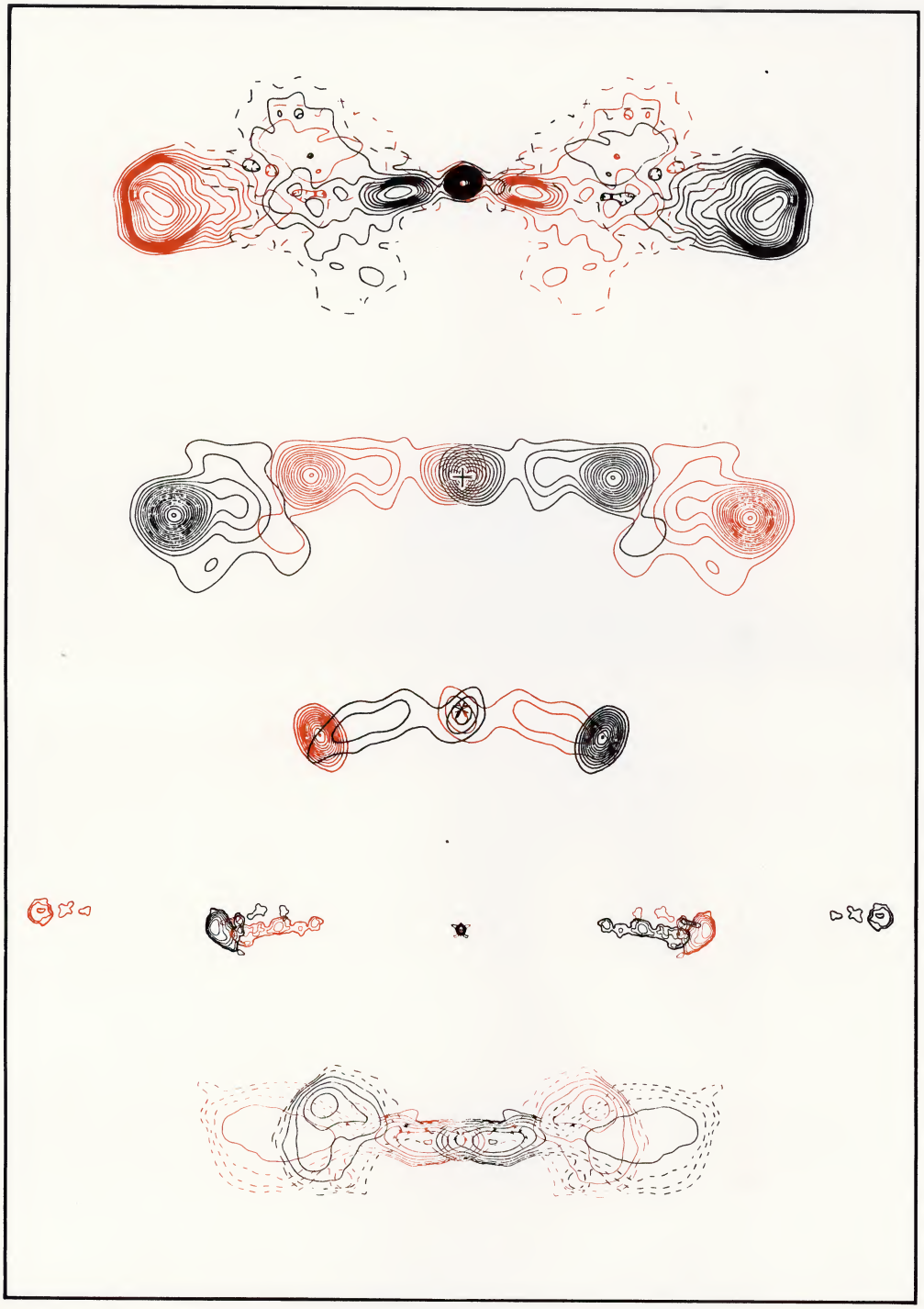

FIG. 2.—Maps specially selected to show the avoidance behavior which is the observational basis for one-sided ejection models. Noise contours (i.e., single contours, not connected to the source) have been removed. Each map has been overlaid by a color copy of itself, flipped 180° around the nucleus. The designations *a–j* correspond to maps ordered top to bottom (first page), top to bottom (second page). Sources are: (*a*) 1004+13, Fomalont 1982. (*b*) 3C 249.1, Pooley and Henbest 1974. (*c*) 3C 280.1, Jenkins, Pooley, and Riley 1977. (*d*) 3C 33.1, Rudnick, Edgar, and Icke 1984. (*e*) 4C 74.17.1, van Breugel and Willis 1981. (*f*) 3C 340, Jenkins, Pooley, and Riley 1977. (*g*) 3C 234, Burch 1979. (*h*) 4C 32.69, Potash and Wardle 1980. (*i*) NGC 6251, Readhead, Cohen, and Blandford 1978. (*j*) 3C 236, Strom, Baker, and Willis 1981.

RUDNICK AND EDGAR (*see* page 74)

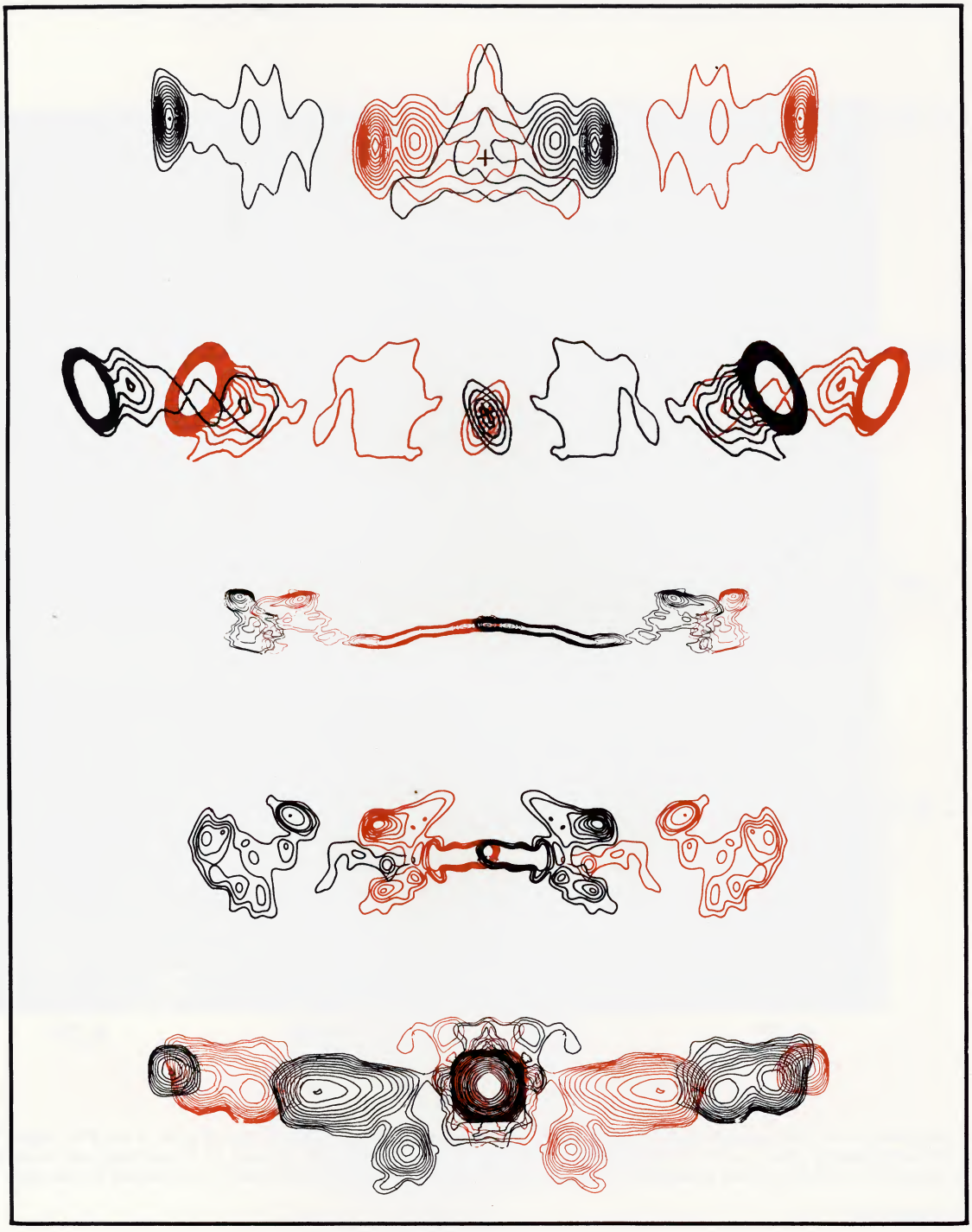

FIG. 2—*Continued*

RUDNICK AND EDGAR (*see* page 74)

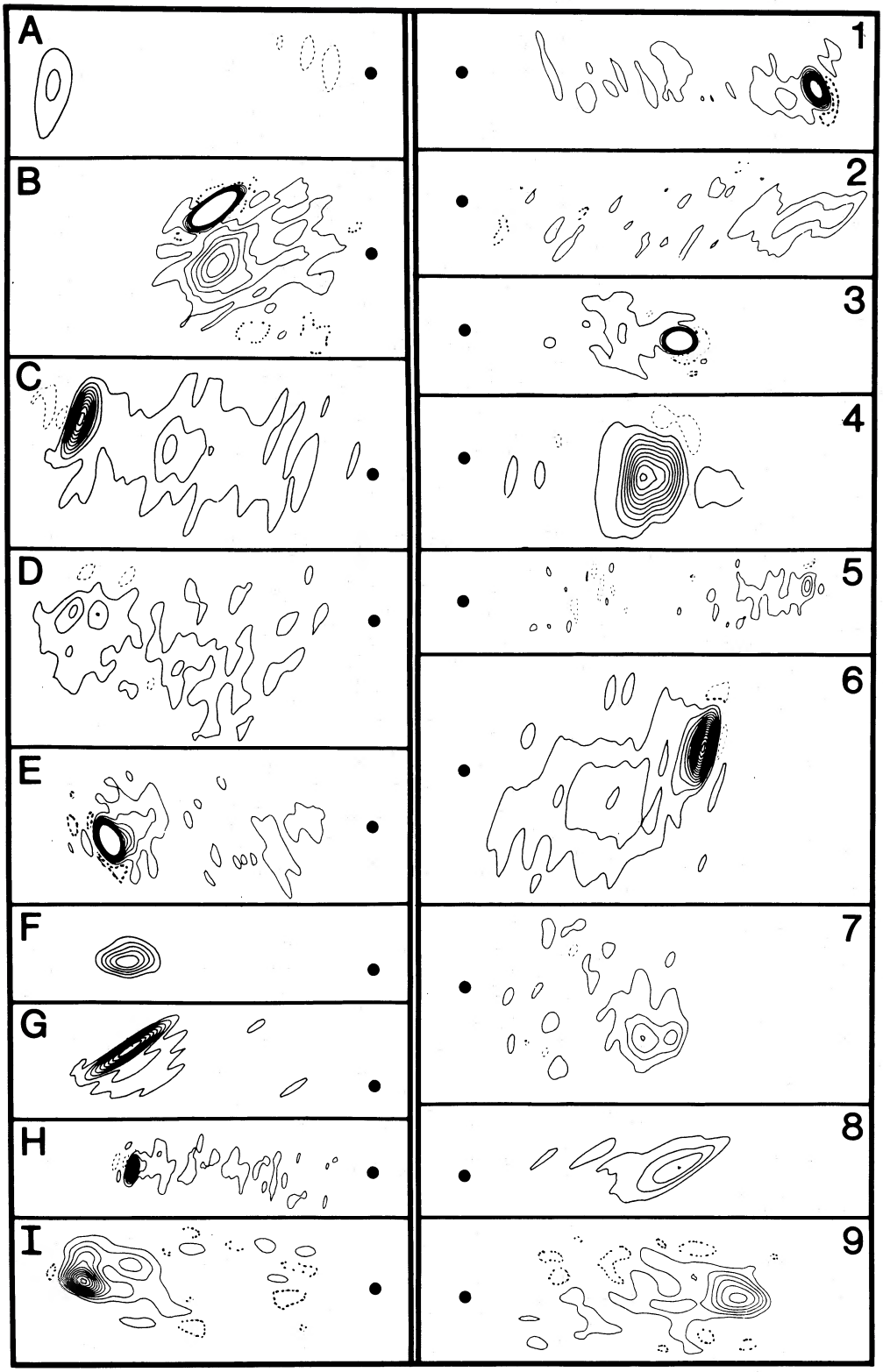

FIG. 1.—Radio maps from Riley and Pooley (1975) have been cut in half, with each half arbitrarily placed in one of the columns. Contours around the central components have been removed. The true pairing is as follows: 3C 152–A4; 3C 300–B2; 3C 79–C6; 3C 357–D7; 3C 234–E1; 3C 386–F3; 3C 109–G8; 3C 284–H5; 3C 223.1–I9.

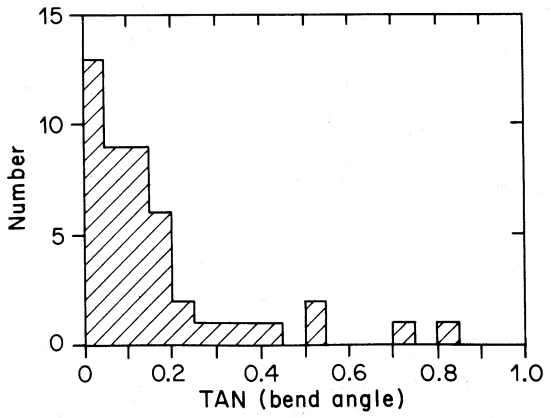

FIG. 3*a*

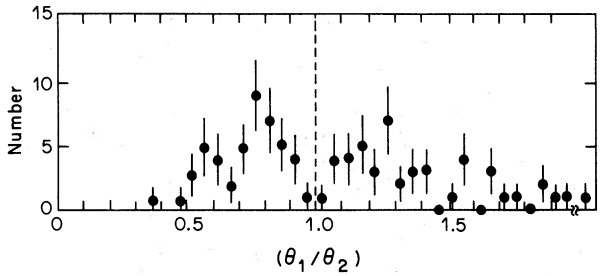

FIG 3*b*

FIG. 3.—The distribution of (*a*) bending angles and (*b*) arm length ratios as discussed in § II*b*, for a sample of 47 QSOs

Should one disregard the often symmetric low surface brightness regions? Many of the best examples of avoidance are clear only when the bright peaks are highlighted (e.g., 3C 192, Högböm 1979; 4C39.04, Hine 1979). Should we ignore the transverse separation of individual components (i.e., away from the source major axis)? Do we look for avoidance of just the peak positions, or of the total extended "components"? The answers to these questions depend on understanding the basic nature of the transport and acceleration of the relativistic electrons; there are no good answers at this time. Turning this around, if we can demonstrate the reality of the avoidance effect, then we will be able to provide answers to some of these basic questions.

b) *Arm Length Ratios*

The simplest test for avoidance is to examine the ratio of distances (θ_1 and θ_2) from the nucleus to the dominant peak on each side of an individual source. To perform this test, we required a sample which (*a*) was of sufficient spatial resolution (we settled, somewhat arbitrarily, on sources more than 4 beamwidths long); (*b*) had well-defined center positions for each source (we required a compact radio component, coincident, within errors, with the optical position); and (*c*) presented the data in a way which did not require subjective judgments. These considerations led us to select all simple double sources more than 4 beamwidths long, with nuclear components, from two quasar surveys on the Green Bank interferometer (Owen, Porcas, and Neff 1978; Potash and Wardle 1979) and two quasar surveys from the WSRT (Miley and Hartsuijker 1978; Fanti *et al.* 1977). The data consisted of models (not maps) of the brightness distributions, which provided us with positions of the three relevant components for each of the 47 sources. For the Green Bank surveys, models at 2695 MHz were used in most cases. In cases of insufficient resolution, where 8085 MHz models were available, the latter were used.

In Figure 3 we show histograms of the arm length ratio (θ_1/θ_2 *and* θ_2/θ_1, each source plotted twice), and the bending angle (see, e.g., Ingham and Morrison 1975 for definition) for this sample. The arm lengths differ, on average, by $\sim 20\%$. This cannot be due to projection effects of bends in the sources, as shown in Figure 4*a*, where we have plotted the expected distribution of arm length ratios, given the observed distribution of bending angles (Fig. 3*a*). This same conclusion was reached earlier by Ingham and Morrison (1975), who stated that, ignoring time delay effects, "a typical *intrinsic* arm difference is 15%–30%."

We have investigated a wide variety of possible arm length determinants, in the attempt to reproduce the distribution in Figure 3*b*. In particular, we are interested in accounting for the dip in the distribution around the (symmetric) value of one. We can test the observations against the hypothesis that the distribution either stays essentially flat or increases monotonically from $(\theta_1/\theta_2) = 0.75$ to 1.0 (as do all our nonavoidance models). This hypothesis is rejected at the 85%–90% confidence level, and provides the strongest objective evidence we have to date that a preferential avoidance effect occurs. A somewhat larger sample of sources compiled by Kapahi and Saikia (1982) shows a clear dip near unity ratio (binning by 0.05) for sources with central components having more than 15% (their division) of the 8 GHz total flux. The lack of a dip at unity for sources with less than 15% cores is almost certainly due to the large position errors for these cores, as examination of the maps shows. Kapahi and Saikia also quote the near-unity arm length ratio of 1.06 for 3C 280.1; this is one of our best avoidance examples (see Fig. 2). Note that Longair and Riley's (1979) best data (their criteria) also show a marginally significant dip towards unity ratio.

Figure 4*b* shows the distribution which would result if the shorter arm length were distributed uniformly from zero to the longer arm length. No dip near unity is predicted. Comparison with the observed distribution does, however, show us that arm lengths *are not random*, but that the two arm lengths are correlated. This statement is valid independent of the distance to each source. Note also the very different shapes of the theoretical distribution in its mapping from the interval (0, 1) to the interval (1, ∞).

There are many parameters which could cause the two arms of an intrinsically symmetric source to differ by $\sim 25\%$ as indicated by Figure 3*b*; these include the velocity of the ejecta, the intergalactic gas density, and the surface mass density of the ejected gas. Other small arm-to-arm length differences should appear because of shape differences and errors in measurement. We may model these "error" type

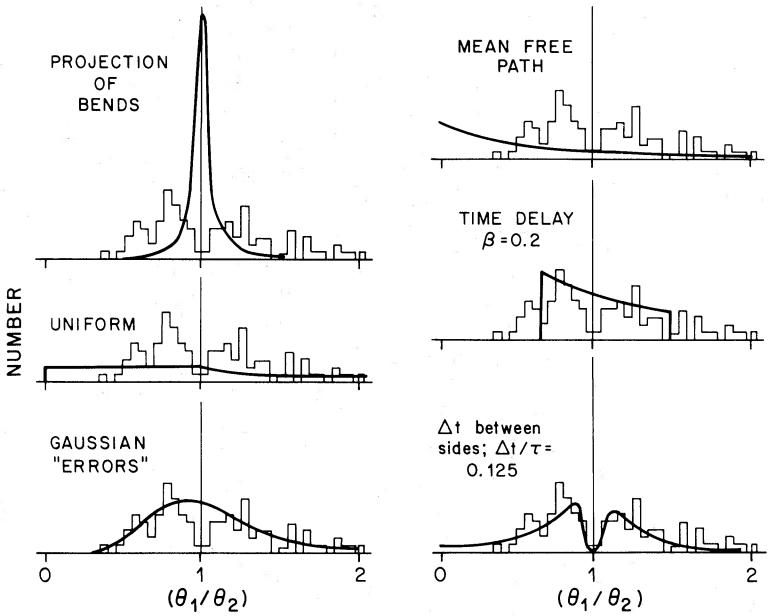

FIG. 4.—Theoretical distributions of arm length ratios (overlaying the observed distribution) under the assumption of symmetric ejection and subsequent smearing due to the listed effects. In the bottom right, we show the theoretical distribution for ejections with identical velocities but separated in time by $\Delta t/\tau$(lifetime) = 1/8.

effects by assuming that the length of each arm of a double source is independently drawn from a population having a well-defined mean and rms scatter around that mean. In Figure 4*c*, we show the arm length ratio distribution which would result for a mean/rms ratio of 3.0. The plotted curve is an analytic approximation, which agrees well with our Monte Carlo calculations. The effect is to broaden the delta function at unity otherwise expected for symmetric sources. However, *it does not create a dip* in the distribution near unity, for errors either parallel to or perpendicular to the source major axis. Our intuitively expected dip can be caused only by an error distribution where the average error is not zero. We therfore reject the class of small random differences between the two arms, whether caused by errors or by other factors, as an explanation for the observed asymmetries.

The location of hot spots is sometimes regarded as the place where an intergalactic cloud or radio relic has been encountered (e.g., Christiansen, Pacholcyzk, and Scott 1977), or where instabilities or shocks develop in a beam (e.g., Blandford and Königl 1979). We may model these behaviors as a mean free path problem, where the probability of hitting a cloud, e.g., at a distance d from the nucleus (and not before), is $P(d) = S^{-1} \exp(-d/S)$, where S is the mean separation between clouds along a straight line. If each arm of the source independently hits a cloud (or develops an instability) at a distance drawn from the above probability distribution, the resulting arm length ratios will be distributed as in Figure 4*d*. Changing S will stretch or compress the distribution; no dip near unity can result, and we reject this class of models.

A symmetric source will appear to have different arm lengths because one arm is usually farther from us than the other, and signals leaving the farther arm reach us from an earlier time than near-arm signals (Mackay 1973). This is a nonrelativistic time delay effect, which scales with $\beta = v_{ej}/c$, and broadens the expected arm ratio delta function over a range $(\theta_1/\theta_2) = [(1+\beta)/(1-\beta)]$ to 1. Longair and Riley (1979) and Katgert-Merkelijn, Lari, and Padrielli (1980) used this analysis to conclude that radio sources have a range of arm velocities around $\beta \sim 0.2$. The shape of the time delay effect is shown in Figure 4*e* for a velocity of $\beta \sim 0.2$; again, there is no substantial dip toward unity value. Nor does a dip result from averaging over any range of velocities.

None of the possibilities discussed above is consistent with our 85%–90% confidence in the avoidance of very symmetric structures. *The key to producing the desired dip in the distribution is "communication" between the two arms of the source; i.e., conditions on the two sides must be preferentially, not randomly different.* A number of possibilities exist. *If* the arms have experienced significant drag, for example, then large scale *gradients* (but not small fluctuations) in the ambient medium could result in a paucity of symmetric sources. A time difference between ejections in the two directions is also possible, and leads to the distribution seen in Figure 4*f*. Further discussion of these and other potential explanations is deferred to § III.

c) Overlap in the Brightness Distributions

Although the distribution of arm length ratios appeared to support our visual impressions, we sought to test more directly the hypothesis that extended regions of emission were preferentially "avoiding" each other, when the two arms were compared. We therefore defined an overlap test as follows:

1. Determine some objective (but arbitrary) contour level above which an arm is defined to be ON, and below which, OFF.
2. Compare the two arms of each source, to see how much of the time they are both ON at the same distance from the nucleus (i.e., overlap of ON regions).

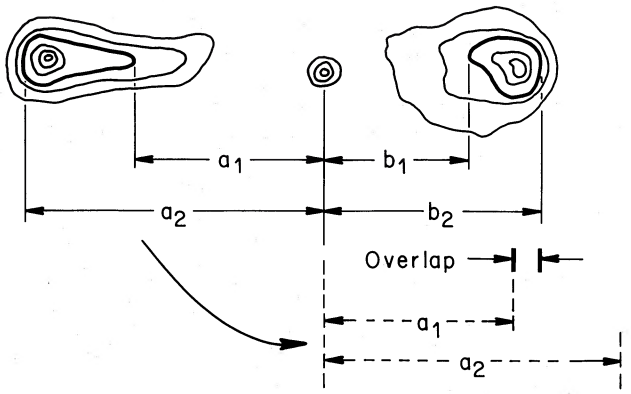

FIG. 5.—Definition of terms for overlap test

3. Contrast the distribution of observed overlaps with theoretical expectations.

We could find no large suitable well-defined sample on which to perform this test. The quasars used in the arm ratio test were mostly dominated by a single component on each arm; a test at lower contour levels would yield little new information. We therefore tried to find as many papers in the literature as possible, which contained high-resolution, reasonable dynamic range ($\gtrsim 20$) maps of samples of radio sources. Forty papers were so identified, containing 64 distinct linear sources (median bending angle = 6°) with central components (≥ 2 closed contours around an optical object), and more than 4 beams along their major axes. For these sources (a list is available to interested readers), we then recorded the distance from the nucleus at which each side turned ON (a_1, b_1; see Fig. 5) and OFF (a_2, b_2), where the longer arm is defined as side a. The third contour level (whatever flux density it represented) was defined as the threshold, for most sources. If the third contour level extended over the complete source (both sides), then the fourth contour level (and so on) was used. If the longer arm of the source was still 100% ON at the level where the shorter arm was 100% OFF, no test was performed. Finally, we defined the normalized overlap as the quantity

$$\phi = \begin{cases} \dfrac{\max\,[(b_2 - a_1), 0]}{a_2} & \text{for } b_1 < a_1 \\ 1 & \text{for } b_1 \geq a_1 \,. \end{cases}$$

The numerator measures the distance over which both sides are simultaneously ON. The denominator is a normalization for source size.

The observed distribution of normalized overlaps is shown in Figure 6*c*. If the avoidance picture is correct, we expect to see a significant excess of zero or very low overlap sources above the number of otherwise predicted. If we assume that the ON region of the shorter side is distributed uniformly from the nucleus to the ON region of the longer side, then the expected overlap distribution is shown in Figure 6*a*. This hypothesis is clearly invalid, as we also know from Figure 4*b*. Note that the theoretical distribution of overlap values depends on the fraction of the source defined to be ON. Our theoretical distribution is thus the sum of the individual source theoretical distributions. We then examined the hypothesis that the two ON regions had a higher than random probability of being close to one another, specifically that the difference (δ) between their respective distances to the nucleus is governed by the linear probability distribution $P(\delta) = 2(1 - \delta/a)$, $0 \leq \delta \leq a$, where a is the longer arm length. This distribution is strictly valid only for point sources, and was modified for each source to properly account for the extent of its ON regions. The resulting distribution is shown in Figure 6*b*.

A χ^2 test shows that Figure 6*b* is an acceptable model for the observed distribution ($\chi^2 = 5.5$ for 10 degrees of freedom). Therefore, although both sides of a source are ON together (according to our arbitrary criteria) only 50% of the time, on average, there is no evidence for further, *preferential* avoidance. We also tested the observations against the hypothesis that there is preferential avoidance—i.e., the component centers are correlated, but never occur within 10% of the same nuclear distance. This is also consistent with the data ($\chi^2 = 7.2$).

We then divided the sources into two luminosity classes, depending on whether they were above or below the median luminosity of $\sim 2 \times 10^{27}$ watts Hz^{-1} ($H_0 = 75$ km s^{-1} Mpc^{-1}). These distributions were also consistent with the above models, and provided no specific evidence for preferential avoidance, either. Note, however, that the preferential avoidance observed in Figure 3*b* has only a small predicted effect in our overlap test; the overlap test is just not powerful enough.

d) Correlation Functions

The overlap test described above makes use of only a limited amount of information from a map. Ideally, we would like to make a full point-by-point comparison of the brightnesses on each arm. As an approach toward this goal, we have made preliminary calculations of arm cross-correlation functions, defined as

$$C(\delta) \equiv \int_0^\infty [B_1(x)B_2(x + \delta)]dx \,,$$

where $B_{1,2}$ is the brightness of an arm, defined along a line at a distance x (or $x + \delta$) from the nucleus. Alternatively, B could

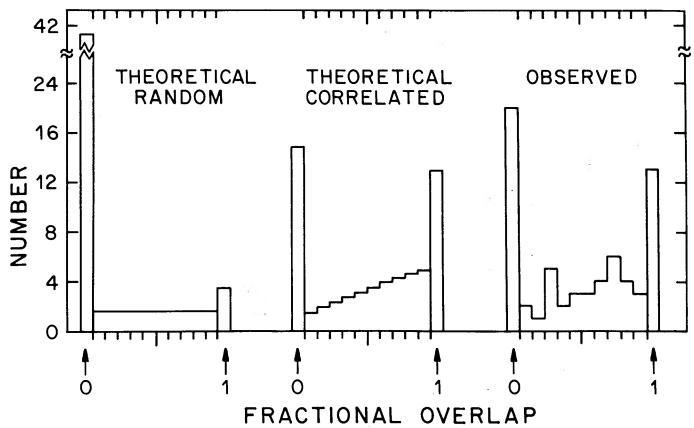

FIG. 6.—The distribution of ON region overlaps as observed, and as predicted for random component positions, and for correlated component positions.

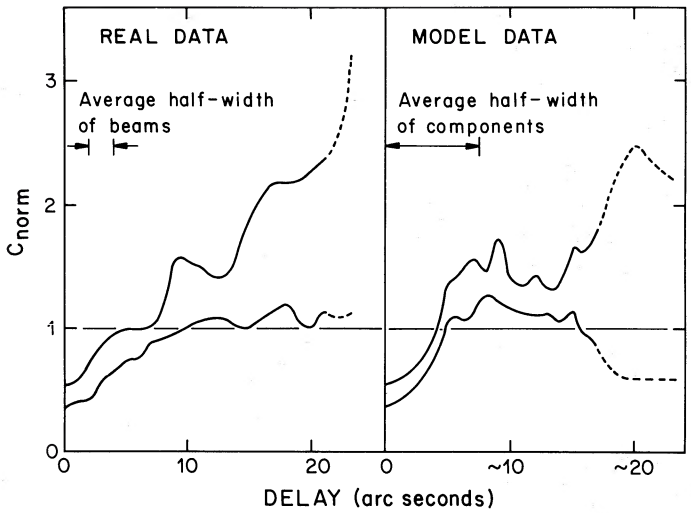

FIG. 7.—Range of correlation functions $C_{norm}(\delta)$ for the middle five sources at each δ, for real data and model data, as described in the text. For the real data, the 1635 MHz maps (Neff 1982*a*) used were 0115+027, 0212+171, 0742+318, 1146−037, 1217+023 (full resolution), 1218+339, 1352+104, 2140−048, and 2201+315.

The model sources were generated as follows. Each side of the model sources consisted of a randomly chosen set of five Gaussian components (a different set on each side) constrained to fall within a fixed range of positions. A randomly chosen low surface brightness component was then added to *both* sides. The random parameters were drawn from a uniform distribution, within the following ranges (unit length ≈ 60″):

Low surface brightness symmetric (1 component): heights: 0–1; position: 0–2; width: 1–2.

High surface brightness, each side independent (5 components): height: 0–10; position 0–1; width: 0.1–0.2. The model sources were then treated identically to the real ones, subtracting a constant from each side and calculating the correlation functions over the distance interval 0–1 (by definition).

be the strip brightness distribution. The quantity δ is the delay, or shift (+ or −), introduced between the arms. For normalization purposes, we also define an autocorrelation function for each source:

$$A(\delta) \equiv \tfrac{1}{2}\int_0^\infty [B_1(x)B_1(x+\delta) + B_2(x)B_2(x+\delta)]dx\ ,$$

and a normalized cross-correlation function $C_{norm}(\delta) \equiv \frac{1}{2}[C(\delta) + C(-\delta)]/A(\delta)$. $C_{norm}(\delta)$ has been symmetrized because we have no current reason to suspect that either arm (e.g., the longer, or the brighter, or the eastern) is special.

The signature of perfect avoidance is $C(0) = C_{norm}(0) = 0$, and perfect symmetry implies $C_{norm}(\delta) = 1$ for all δ. Since low surface brightness features are often symmetric, avoidance of high surface brightness features may still not result in $C_{norm}(0) = 0$. Instead, one must look for a *dip* at $C_{norm}(0)$, which may be superposed on a fairly level background.

As few maps are available in the form of brightness profiles, we used a small sample (since conversion from contour maps is so painful) of reasonably complex sources, with central components, chosen in an unbiased way. In her thesis, S. Neff (1982*a*) mapped 60 quasars, 10 of which had complex brightness distributions which were not adequately described by a small number of model components, and which she consequently displayed as maps (four of these are published in Neff 1982*b*). These sources were not known or selected to have any particular symmetry or asymmetry characteristics; we chose this sample (see names in Fig. 7 notes) for our initial, exploratory correlation analysis. We rejected one source (1222+216) because of its large bending angle (~80°). For each of the others, we first drew (by hand) the straight (or curved, as necessary) line which intersected as many brightness peaks as possible. These lines defined the major axis for each source, and were *forced* to be symmetric. Contour level crossings were measured as a function of length along the major axis, the data were plotted, smooth curves drawn through them by hand, and the curves resampled at equal intervals. These (re)samples served as our estimates of the brightness profiles, which were normalized to meet the condition $\sum B^2(i) = 1$, for each arm independently, and then used to calculate the correlation functions. This somewhat arbitrary choice of normalization was made to equalize the contribution of the two arms.

Only two of our nine sources showed strong symmetry [$C_{norm}(0) \approx 1$]. Figure 7*a* shows the range of $C_{norm}(\delta)$ for the middle five of the nine measured sources, at each δ. In order to interpret these correlation functions, we generated a set of model sources, and performed the same correlation analysis on them (see Fig. 7*b*). Our primary objective was to duplicate, with our model sources, the features of the true correlation function. For example, do we need *preferential* avoidance to reproduce the low values of $C_{norm}(0)$, or merely a random distribution of flux on each side of a source? Details of the model source generation are found in the notes to Figure 7. The full set of $C(\delta)$ and $C_{norm}(\delta)$ plots can be sent upon request.

The true and model data sets both had median values of $C_{norm}(0) \approx 0.45$, indicating that ~45% of the flux was distributed symmetrically, with the remaining ~55% distributed in different places on the two sides. The behavior of $C(\delta)$ and $C_{norm}(\delta)$ for $\delta \neq 0$ is not easily interpreted. If one side were simply the *delayed* version of another (as the time delay or velocity difference models predict), then $C(\delta)$ would show a single strong peak (reaching 1.0) for the proper delay. The data are, in general, not so simple. For now, we merely note that the model data are in good agreement with the true data in the values of $C_{norm}(0)$, the rise in C_{norm} for $\delta > 0$, and the spatial frequency components present. We conclude that the current data are consistent with our models of a *random* distribution of flux over an average of ~5–10 independent beam areas scattered around the same position on each side.

In order to pursue a clear signature of the proposed "flip-flop" or preferential avoidance behavior, we need (1) a spatial filtering scheme (i.e., a defining brightness or spatial scale) to separate low and high surface brightness contributions to the symmetric flux; and (2) a large sample to distinguish random from preferential avoidance (as in § II*b*).

III. PREFERENTIAL AVOIDANCE MODELS

In order to explain the scarcity of symmetric sources (§ II*b*) and the structures in Figure 2, parameters for one arm must be preferentially, not randomly, different from those on the other arm. Although the evidence may not yet be compelling, we wish to explore the possible causes of preferential avoidance. The parameters available for this are (*a*) initial velocity; (*b*) drag force; and (*c*) time of ejection. Each is discussed below.

a) Slingshot Model

One physical model already exists which predicts preferentially different velocities for the two arms. This is the slingshot model (Saslaw, Valtonen, and Aarseth 1974), whose asymmetry properties have been specially addressed by Valtonen (1979). The critical concept is that slingshot ejection takes place most readily when the interacting nuclear masses differ from one another; conservation of momentum then forces the ejecta on the two arms to have *preferentially* different velocities. With a suitable choice for the nuclear mass distribution, the slingshot model is consistent with the evidence of § II*b*. However, sources should then appear essentially the same on each side, differing only in scale between sides.

b) Galaxy Motion/Different Drags

A preferential difference in drag force between the two sides could arise from large-scale gradients in the intergalactic medium. To see what effect this could have on the arm length ratio, θ_1/θ_2, we assumed that constant cross section blobs had been stopped by a medium having a linear density gradient across the parent galaxy. We found the following rough empirical relation:

$$\left|1 - \left(\frac{\theta_1}{\theta_2}\right)\right| \approx 0.25 \frac{\theta_1 + \theta_2}{D},$$

where D is the distance over which the density changes by a factor of 2. Thus, one could reproduce the observed ratio distribution by a suitable range of density (drag) gradients.

As an alternative mechanism, different initial velocities with respect to the external medium will arise when the direction of the parent galaxy motion through the medium is not perpendicular to the ejection direction. Note that this is a drag effect, not one of initial velocity;[1] for an inconsequential external medium, the entire system will move with the galaxy's velocity, preserving its initial (a)symmetry. However, drag forces probably are important, because of the observed bending of most sources. (Alternatively, acceleration of the nucleus, as in orbital motion—e.g., 3C 31, Blandford and Icke 1980—could also cause bending.) If the bends are drag induced, can these drag forces also account for the arm lengths being preferentially different? This effect is unlike the random ones discussed in Section II.B, because if there is a component of the galaxy's velocity in the direction of one arm, then the velocity of that arm with respect to the external medium will be *prefentially* larger than that of the other arm.

In order to estimate the magnitude of this differential drag effect, we used the Christiansen (1969) deceleration plasma blob model as extended by Jaffe and Perola (1973) for use in head-tail sources. As discussed by Rudnick and Burns (1981), the results do not change significantly for models using beams. We considered fixed radius, and expanding (pressure equilibrium) and contracting blobs. Expansion might be enhanced, if heating is important (Eilek 1979), while contraction can result if synchrotron cooling dominates (Christiansen, Rolison, and Scott 1979). As detailed below, an external observer sees a bent, asymmetric double.

For simplicity, we restrict our attention to the case where the angle between the ejection and galaxy velocities takes on its median value of $2/\pi$ radians. We may reduce all the unknown variables to two independent quantities, which we choose for convenience to be $v \equiv v_{\rm ejection}/v_{\rm galaxy}$ (the velocity ratio) and $\tau \equiv 2t/(T_1 + T_2)$, where t is the age of the source, and T_1 and T_2 are the stopping times of the two arms, respectively. Figure 8 shows the loci of constant bending angle (b) and constant arm length ratio (θ_1/θ_2), in the parameter space defined by v and τ, for the constant cross section case. (The other cases are qualitatively similar.) The braces delineate the region in which the middle half of the observed bending angles falls, for the sample of § II*b*. Within this region, an otherwise symmetric source *could* be preferentially distorted to have $|(\theta_1/\theta_2) - 1| \lesssim 0.1$.

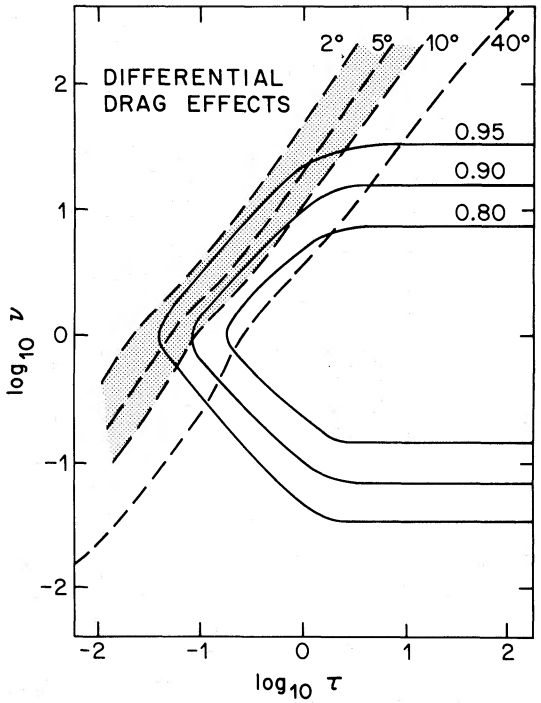

FIG. 8.—Predicted values of bending angle (*dashed*) and arm length ratio (*solid*) due to *differential* drag forces on blobs moving through an intergalactic medium. τ is the ratio of elapsed to stopping time of the blobs; v is the ratio of blob ejection to galaxy velocities. The shaded region indicates typical observed bending angles. All calculations were done for a characteristic angle of $2/\pi$ between galaxy and ejection velocities.

W. Christiansen has also suggested (privately) that the observed differences in brightness between the two sides of a source could signify differences in the heating/cooling rates of the two plasmas. If drag is important, then the concomitant differences in cross section would lead to asymmetric structures.

We conclude that differential drag could cause the observed depletion of sources at $(\theta_1/\theta_2) = 1$, for certain restricted ranges of v and τ (which may be physically reasonable), or external density gradients, or nonadiabatic dynamics. Note however, that nearly all sources must be so affected to produce the dip in Figure 3*b*, even those with small bending angles or those isolated spatially. Also, contrary to observations, these arguments suggest that the two sides should differ only in scale, not overall structure.

[1] The analysis of Macklin (1981) appears to make this error.

c) *Nonsimultaneous Ejection*

A short-duration ejection of material which occurs in one direction, followed at a later time by an ejection in the opposite direction, can lead to the specific avoidance discussed in § II*b*. Figure 4*f* shows the distribution of (θ_1/θ_2) which would result if the ages T of radio sources were distributed according to $P(T) = \tau^{-1} \exp(-T/\tau)$, for some characteristic lifetime τ, and if the time interval between ejections were $\Delta t = \tau/8$. The requisite conditions are that the ejection velocities be the same on both sides and that little or no drag occur (see details in § IV). *This model also predicts that ~12% of radio sources should be one-sided.*

The nonsimultaneous ejection model enjoys a distinct advantage over those discussed above because it is consistent with the observed structures in Figure 2. In this interpretation, when strong emission is observed on one side at a distance d from the nucleus, it tells us that at a time $t = d/v_{ej}$ ago, the nuclear engine was ejecting material on that side. At this point (without a physical model to guide us), there is no reason why the strength or length of ejection should be the same at all times or similar between the two sides. Therefore, no problem is raised by sources whose structures are very different on the two sides.

By contrast, the intrinsically symmetric models discussed in §§ II*a* and III*b* have great difficulty explaining the appearance of features such as one-sided jets. Numerous attempts have been made to explain these asymmetries (see, e.g., van Groningen, Miley, and Norman 1980; Rees 1982) without convincing results. On the basis of the subjective visual evidence of avoidance, such as illustrated in Figure 2, and apparent for many other sources, we tentatively accept the single-sided ejection (or flip-flop, following Wiita and Siah 1981) picture as our working hypothesis.

The flip-flop model is not without difficulties. Most serious is that in its simplest form it embodies no explanation for the high degree of symmetry which also is seen in most sources. However, because of its potential importance, we discuss below the implications of the flip-flop picture, and several suggestions about how it can be physically realized.

IV. IMPLICATIONS OF ONE-SIDED EJECTION

a) *Physical Parameters of Extended Emission*

We assume, in this section, that the flip-flop picture is correct, and discuss the constraints thus imposed on (*a*) ejection velocity, (*b*) differences in ejection velocity, (*c*) drag, (*d*) differences in drag, (*e*) the nature of low surface brightness features, jets, and hot-spots. For the purposes of calculation, we will assume that the data in § II*b* indicate a range of time delays between the alternate side ejections with a characteristic value of 0.25× source age. The question we now ask is: What factors could cause our observed avoidance to be washed out?

Ejection velocity is the simplest parameter to consider. The time delay effect discussed in § II would also broaden the observed (θ_1/θ_2) distribution for nonsimultaneous ejection, and cause the dip near unity to be filled in. Figure 9 illustrates this effect for three different velocities. Values of $\beta(= v_{ej}/c) \gtrsim 0.12$ fill in the dip and are therefore rejected. Ejection velocities $\beta \approx 0.1$ could be responsible for the breadth of the (θ_1/θ_2) distribution, if the same fractional time between ejections was true for all sources.

Random differences in ejection velocity would similarly cause the observed avoidance to disappear. For the sample as a whole, velocity differences $\gtrsim 20\%$ between the two ejections in a source are not allowed. It is inappropriate at this point to refine these constraints further, since they depend on the unknown shape of the radio source age or size distribution.

In the case where *drag* has essentially stopped the advance of radio source components, then distance from the nucleus is no longer an indicator of time of ejection. A sample of sources with an interval between ejections which is ~0.25 × the age (T) of the source, must have $T/\tau_{stop} \lesssim 1$, where τ_{stop} is the stopping time of the source. For expanding blobs of plasma, we therefore have (e.g., Jaffe and Perola 1973) $\tau_{stop} \approx (M/\rho R^2 v_{ej}) \lesssim 1$, where R is the blob radius, ρ is the external gas density, and M is the mass of the blob. Similar constraints exist for collimated motion. However, the standard analysis of *beam* advance speed, calculated through a drag-incurred

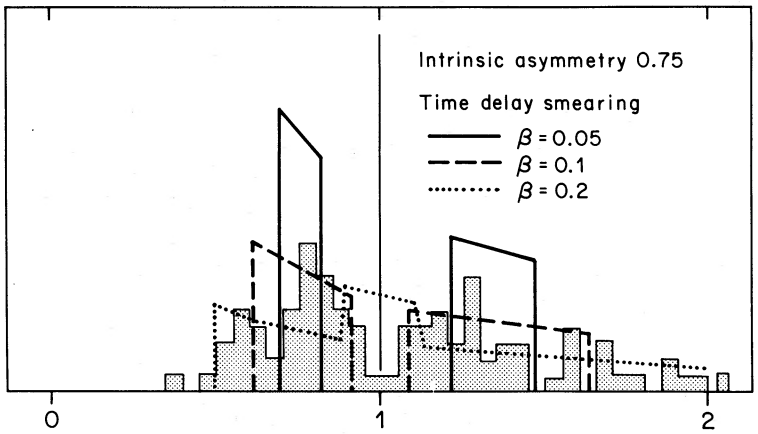

FIG. 9.—Predicted distributions of arm length ratios, assuming ejections with a time difference yielding unperturbed $(\theta_1/\theta_2) = 0.75$, then smeared out by the time delay effect, for three different velocities. The observed distribution is shown shaded.

terminal velocity, is not appropriate here (see discussion below).

When $T/\tau_{stop} \ll 1$, then $\theta_i = v_i T_i$ is independent of τ_{stop}. However, if $T/\tau_{stop} \sim 1$, as allowed by the above arguments, then θ_i does depend on τ_{stop}, and *small differences* ($\sim 25\%$) *in drag* (τ_{stop}) from one side to the other would fill in the dip in the (θ_1/θ_2) distribution. Since the cross section (the one observable quantity in τ_{stop}) may easily differ by a factor of 4 between sides of a given source, we consider it unreasonable to conclude that the two values of τ_{stop} are equal. This would require an adjustment of the mass or external medium density to equalize the τ values, for which there is no physical basis.

These constraints lead us to a lower limit for the density of nonrelativistic material embedded in the source. Similar analyses have often been applied in the past, but the justification of each step is different here. We first note that $v_{ej}/c \lesssim 0.12$, as argued above. The *minimum* pressure in typical hot spots is $\sim 10^{-11}$ ergs cm^{-3}. For ram pressure confinement (supported by, e.g., Dreher 1981, in his analysis of high resolution maps), this implies that the external density $\rho_{ext} \gtrsim 10^{-28}$ g cm^{-3}. On the basis of the observed avoidance, we calculated that $t/\tau < 1$. Together with an internal "equation of state" (for simplicity, we used Jaffe and Perola's 1973 expanding blobs), we find

$$\rho_{int} \gtrsim 2 \times 10^{-26} \text{ g cm}^{-3}, \quad \text{or} \quad n_{int} \gtrsim 0.02 \text{ cm}^{-3}.$$

For many hot spots, these limits would be considerably higher. This is $\sim 10^6$ times the density of relativistic material, and therefore dominates the dynamics of the radio source. If the thermal material is cold, $n_{int} kT_{int} < U_{rel}$ (the relativistic energy), then the relativisitic material will dominate the internal dynamics. Otherwise, we find that for pressure balance of unstopped material $R/L > v_{th}^2/v_{ej}^2$, where L is the arm length, and v_{th} is the internal thermal velocity. From the expansion and ejection motions, however, $R < v_{th} t$ and $L = v_{ej} t$, so $R/L < v_{th}/v_{ej}$. Therefore, taking, for example, $R/L \sim 1/50$, we find $(1/50) < v_{th}/v_{ej} < (1/50)^{1/2}$. We note that these limits, which apply only to constant cross section flows, are *consistent* with the velocity and density estimates in some jets (e.g., Saunders *et al.* 1981). However, the requirement $n_{int} \gtrsim 0.02$ cm^{-3} is inconsistent with typical hot spot depolarization limits (e.g., Hargrave and McEllin 1975), and the thermal material cannot be uniformly mixed with the relativistic plasma there. None of these arguments or conclusions is really new; we present them here because our perspective is different on their justification.

Based on these constraints, we arrive at the following description of extended radio sources:

1. The radio-emitting material is ejected at a velocity between 3×10^2 (escape velocity) and $\sim 3 \times 10^4$ km s^{-1}, in one direction at a time. The velocities in subsequent ejections are constant to within $\sim 20\%$.

2. The relativistic material is carried along by a much more massive quantity of cold matter.

3. The direction of ejection switches, sometimes after only a short time, and the material on the switched-off side continues moving away from the nucleus as an isolated component. The emission falls off rapidly after the material is stopped.

4. The direction of ejection sometimes stays fixed for a substantial period, resulting in a jetlike structure.

5. A hot spot develops at each leading edge of the source. However, since the hot spot is not stopped (i.e., continues to move out at close to its original velocity) and since all subsequent material comes out at approximately the same velocity, *there is no continual supply of energy from the nucleus.*

6. Some of the relativistic (and cold?) matter is stripped from the main flow (e.g., Nepveu 1979) and stopped with respect to the external medium, providing the observed symmetric underlying structures. Alternatively, symmetric structures would arise if there is not 100% modulation of the ejection strength, i.e., if the OFF side is not completely off.

Point (5) requires further comment because it departs so strongly from the conventional wisdom (Blandford and Rees 1974). The localized particle acceleration required by observations (e.g., Rudnick *et al.* 1981; Willis and Strom 1978) must be energized from the initial ejecta, not by subsequent resupply. It also implies that the dynamics (along the ejection direction) of individual components are independent, and do not depend on continuous flows, magnetic fields originating from the nucleus (Chan and Henriksen 1980), or channels (Christiansen 1973). However, each of these factors may well influence the details of the radio brightness, if not the overall dynamics. In our model the *collimation* of long jets cannot involve any communication along the jet, but could be solved by external forces such as preexisting channels or density gradient focusing (Sanders 1983). If collimation can occur independently at each point in the jet, then collimated "pieces of jets" should exist, well apart from the nucleus. Studies of two such pieces of jets are now in progress; one of these 3C 33.1, is shown in Figure 2.

The reader should remember that all of these conclusions are based on the assumption of one-sided (alternating) ejection.

b) The Nature of the Nuclear Engine

Most theoretical efforts at understanding the nuclear engine have concentrated on its bidirectionality (e.g., Scheuer and Readhead 1979). In fact, this assumption of symmetry has led to many numerical calculations (e.g., Norman *et al.* 1982) being done on only half of the source, not allowing for any side-to-side differences. More recent discussions of asymmetric conditions near the nucleus will be discussed below.

First, however, we look at a simple empirical (i.e., not physical) source simulation model to see whether the direction-switching and ejection mechanisms can be periodic functions, running independently of each other. This is relevant to classes of physical models for which the ejection and switching regulators derive from different aspects of the source. The data for comparison are the arm length ratios discussed in § II*b*. Our simulation used two independent cycles: a "left-right" cycle and an "ejection" cycle. The left-right cycle determines on which side of the source material can be ejected. It is a square-wave function normalized to a period of 1. The ejection cycle determines when the nuclear engine is allowed to eject matter. It is a periodic function which is on for a fraction α of its period B, and off for the remainder of the time.

The (θ_1/θ_2) statistics for all possible sources that can be created from these two independent cycles were computed. We looked only at double sources. This is equivalent to assuming that the particle lifetime is approximately equal to the ejection period B, so that earlier ejections are invisible, and that only a small number of one-sided sources will be produced.

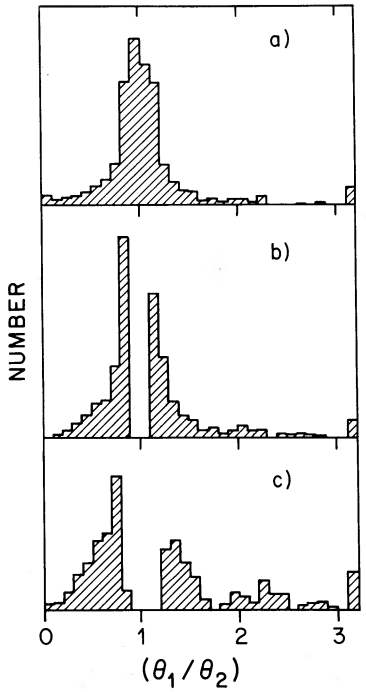

FIG. 10.—Distribution of arm length ratios for empirical models of periodic, independently running side-switching and ejection mechanisms. The fractional ON time, and the ejection period (in units of the side-switching period), are respectively (*a*) 0.12, 4.3; (*b*) 0.2, 2.3; and (*c*) 0.38, 1.3.

The general shape of the observed (θ_1/θ_2) distribution can be reproduced for an ejection cycle with a fraction on-time of $0.2 \lesssim \alpha \lesssim 0.3$ with a period of $1.5 \lesssim B \lesssim 3$. A typical well-fitting distribution is given in Figure 10*b*. Increasing the ejection period tends to produce more symmetrical sources, while changing the fractional ON time tends to produce more asymmetrical sources, as shown in Figures 10*a* and 10*c*. Our conclusion from this analysis is that periodic, independently running, switching and ejection mechanisms can account for the observations but only for a narrow range of duty cycles, relative periods, and particle lifetimes, which may not be physically reasonable.

Wiita and Siah (1981) have examined the behavior of central plasma sources which are offset from the center of their flattened confining cloud (i.e., a perturbation of the standard Blandford and Rees 1974 model). Wiita and Siah find that "if the source of plasma is even slightly displaced with respect to the center of the confining gas cloud, a strongly asymmetrical cavity is formed, leading toward single jet formation or the emission of a string of bubbles in one direction." They suggest that orbital motion of the nuclear engine around the center of the confining cloud could provide the switching necessary to produce two-sided sources, and note that NGC 6251 shows the "avoidance" type structure. Icke (1982) has criticized the orbital mechanism on the grounds that orbital times $\tau \sim (G\rho)^{-1/2}$ are far too short to produce the long jets, such as in NGC 6251.

An alternative model for one-sided structures has been proposed by Icke (1982). He suggests that confinement of the central plasma source contains dynamic, as well as static, contributions. If the external confining flow is set up by entrainment in the initial Blandford-Rees type jet, then an instability develops whereby the stronger jet can actually pinch off the weaker one, or cause it to go subsonic. Whether or not the flow will later switch directions, or whether the engine will stop and restart in either direction, are still open questions.

Shklovsky (1982) considers the question of momentum conservation in one-sided ejections. His conclusion is that the original energy source, a massive accreting black hole, can escape from the nucleus. In typical steep-spectrum sources, the central component can reappear when another black hole replaces the ejected one.

In addition to providing a physical understanding of one-sided flows, any theoretical model must still deal with the overall symmetry of radio galaxies. This involves more than noting that two ejection directions are *a priori* equally likely. It involves understanding the often symmetric low surface brightness material (which might just be stopped plasma) and, more important, why so many sources are dominated by (*almost* equidistant) single components on each side of the nucleus.

V. SUMMARY AND CONCLUDING REMARKS

We have analyzed the asymmetries in various samples of radio galaxies and QSOs and arrived at the following conclusions:

1. The distribution of arm length ratios indicates a preferential difference between the two arms of each source, which cannot be explained by random fluctuations, projection, or time delay effects.

2. Explanations for the above distribution include slingshot model velocity differences, differential drag due to galaxy motion, and separate ejection times for each arm.

3. If radio sources are powered on only one side at a time (as the subjective examination of many maps indicates), then each lobe (*a*) has the same velocity ($\lesssim 0.1c$) to within 20%, (*b*) is dominated in momentum by nonrelativistic material, and (*c*) contains its own energy source, with jets representing merely a long-term ejection, not a power source for structures downstream.

4. The overlaps between structures on opposite sides of sources are consistent with a broad distribution of component separations, but do not provide any specific evidence for avoidance, so far as we have been able to test it.

5. Correlation functions between the two arms indicate that the flux density is (at least) randomly distributed within certain boundaries on each side, but again do not provide any specific evidence for avoidance, so far as we have been able to test it.

6. Models which seek to explain both the observed symmetries and asymmetries will probably require a narrow range of values for the switching, ejection, and particle lifetime scales, perhaps suggesting a physical connection between the switching and ejection mechanisms.

We have so far eschewed any discussion of one-sided sources. These may well be the best examples of one-sided ejections. However, limited dynamic range may be a confusing factor, as recent observations of 3C 293 (Fomalont 1982) show. In addition, there is the intriguing observation by Kapahi (1981) that one-sided sources have preferentially stronger

central components, a fact that does not fit naturally, at this point, into our flip-flop picture.

Kapahi (1981), and Kapahi and Saikia (1982) (among others) suggest that the brightness of the central (and perhaps extended) components may be due to relativistic beaming, which appears well documented on smaller scales (Kellermann and Pauliny-Toth 1981). However, large-scale relativistic beaming does not work well in individual cases (see, e.g., Potash and Wardle 1980; Saikia and Wiita 1982) or in statistical tests (Saikia 1981; Gopal-Krishna 1980). If relativistic beaming of central components in extended sources does occur commonly, then our sample in § II*b* is biased against sources which are transverse to the line of sight. These are the sources which would suffer least from the time delay asymmetries, and our conclusions regarding the arm length ratio distribution would be invalid. This problem was pointed out to us independently by M. Reid and V. Kapahi. However, low-accuracy positions for weak central components (such as those analyzed by Kapahi and Saikia) preclude checking for this effect, at present.

It is not clear how the "twin-jet" low luminosity radio galaxies fit into our flip-flop picture. Some of these (e.g., NGC 315, Willis *et al.* 1981; NGC 1265, Owen, Burns, and Rudnick 1978) clearly show "avoidance" of their peaks, while having substantial underlying symmetric brightness distributions. Others (e.g., B2 1323+31, Ekers 1982) are embarrassingly symmetric. A very fast switching cycle could obscure avoidance behavior, given our limited resolution. Recent VLBI observations by Linfield (1981) and especially Kellermann and Pauliny-Toth (1981) appear to support avoidance on parsec scales. From pressure confinement and other arguments, Linfield (1982) concludes that radio galaxy VLBI jets are intrinsically asymmetric. The observation of twin jets or symmetric structures around a central component on a VLBI scale would be a serious argument against the flip-flop model.

The observed correlation of misalignment (bending) angle with arm length asymmetry (Macklin 1981; Kapahi and Saikia 1982) is not an automatic result of the flip-flop model. However, it could result if there were a substantial misalignment due to offsets from galaxy orbital motion; younger (smaller) sources would appear fractionally less asymmetric and more bent.

Analysis of arm length ratios for larger samples would clearly be useful, to tighten the statistics and guard against the bias toward sources along the line of sight. More sophisticated analyses (perhaps two-dimensional) of the brightness distributions, such as our overlap or correlation calculations, need to be pursued. Independent of the flip-flop picture, these analyses would provide important information on the symmetric and asymmetric aspects of source structures, constraining possible brightness producing mechanisms, and their dependence on both internal and external conditions.

Finally, a clean test for avoidance may not yet be possible, given our limited knowledge of the causes of various observed structures. We urge the reader to look at any available maps, and see how prevalent the avoidance of high surface brightness features is (as in some of the best cases of Fig. 2). At the very least, we should keep in mind the very limited sense in which classical doubles are symmetric.

Thanks to many of our colleagues for discussions of the ideas discussed here and criticisms of the text. We especially thank V. Icke, A. H. Bridle, R. Ekers, M. Reid, R. Sanders, T. Jones, V. Kapahi, and the referee, W. Christiansen, for their input. Thanks also to G. Pooley, E. Fomalont, W. van Breugel, R. Strom, J. Wardle, S. Burch, S. Neff, and T. Readhead for use of their maps. G. Miley's longstanding emphasis on symmetries helped inspire our initial questions about asymmetric structures. This work was supported in part by NSF grant AST 81-14737.

REFERENCES

Birkinshaw, M., Laing, R. A., and Peacock, J. A. 1981, *M.N.R.A.S.*, **197**, 253.
Blandford, R. J., and Icke, V. 1978, *M.N.R.A.S.*, **185**, 527.
Blandford, R. D., and Königl, A. 1979, *Ap. Letters*, **20**, 15.
Blandford, R., and Rees, M. J. 1974, *M.N.R.A.S.*, **169**, 395.
Bridle, A. G. 1982, *IAU Circ.*, No. 97, p. 121.
Burch, S. F. 1979, *M.N.R.A.S.*, **186**, 293.
Chan, K. L., and Henrikson, R. N. 1980, *Ap. J.*, **241**, 534.
Christiansen, W. A. 1969, *M.N.R.A.S.*, **145**, 327.
———. 1973, *M.N.R.A.S.*, **164**, 211.
Christiansen, W. A., Pacholcyzk, A. G., and Scott, J. S. 1977, *Nature*, **266**, 593.
———. 1982, *IAU Circ., No. 97*, p. 51.
Christiansen, W. A., Rolison, G. G., and Scott, J. S. 1979, *Ap. J.*, **234**, 456.
Dreher, J. W. 1981, *A.J.*, **86**, 833.
Eilek, J. 1979, *Ap. J.*, **230**, 373.
Ekers, R. D. 1982, *IAU Circ.*, No. 97, p. 465.
Fanti, C., *et al.* 1977, *Astr. Ap. Suppl.*, **28**, 351.
Fomalont, E. B. 1982, *A.J.*, **86**, 1294.
Gopal-Krishna 1980, *Astr. Ap.*, **86**, L1.
Hargrave, P. J., and McEllin, M. E. 1975, *M.N.R.A.S.*, **173**, 37.
Hine, R. G. 1979, *M.N.R.A.S.*, **189**, 527.
Högbom, J. A. 1979, *Astr. Ap. Suppl.*, **34**, 129.
Icke, V. 1982, *Ap. J.*, **254**, 517.
Ingham, W., and Morrison, P. 1975, *M.N.R.A.S.*, **173**, 569.
Jaffe, W., and Perola, G. C. 1973, *Astr. Ap.*, **26**, 423.
Jenkins, C. J., Pooley, G. G., and Riley, J. M. 1977, *Mem. R.A.S.*, **84**, 61.
Kapahi, V. K. 1981, *J. Ap. Astr.*, **2**, 43.
Kapahi, V. K., and Saikia, D. J. 1982, preprint.
Katgert-Merkilijn, J., Lari, C., and Padrielli, L. 1980, *Astr. Ap. Suppl.*, **40**, 91.
Kellermann, K. I., and Pauliny-Toth, I. I. K. 1981, *Ann. Rev. Astr. Ap.*, **19**, 373.
Linfield, R. 1981, *Ap. J.*, **244**, 436.
———. 1982, *Ap. J.*, **254**, 465.
Longair, M. S., and Riley, J. M. 1979, *M.N.R.A.S.*, **188**, 625.
Mackay, C. D. 1973, *M.N.R.A.S.*, **162**, 1.
Macklin, J. T. 1981, *M.N.R.A.S.*, **196**, 967.
Miley, G. K. 1971, *M.N.R.A.S.*, **152**, 477.
———. 1980, *Ann. Rev. Astr. Ap.*, **18**, 165.
Miley, G. K., and Hartsuijker, A. P. 1978, *Astr. Ap. Suppl.*, **34**, 129.
Neff, S. G. 1982*a*, Ph.D. thesis, University of Virginia and NRAO.
———. 1982*b*, in *IAU Symposium 97, Extragalactic Radio Sources*, ed. D. S. Heeschen and C. M. Wade (Dordrecht: Riedel), p. 137.
Neff, S. G., and Rudnick, L. 1980, *M.N.R.A.S.*, **192**, 531.
Nepveu, M. 1979, *Astr.*, **79**, 40.
Norman, M. L., Smarr, L., Winkler, K.-H. A., and Smith, M. D. 1982, *Astr. Ap.*, **113**, 295.
Owen, F. N., Burns, J. O., and Rudnick, L. 1978, *Ap. J. (Letters)*, **226**, L19.
Owen, F. N., Porcas, R. W., and Neff, S. G. 1978, *A.J.*, **83**, 1009.
Pooley, G. G., and Henbest, S. N. 1974, *M.N.R.A.S.*, **169**, 477.
Potash, R. J., and Wardle, J. F. C. 1979, *A.J.*, **84**, 707.
———. 1980, *Ap. J.*, **239**, 42.
Readhead, A. C. S., Cohen, M. H., and Blandford, R. D. 1978, *Nature*, **272**, 131.
Rees, M. J. 1982, in *IAU Symposium 97, Extragalactic Radio Sources*, ed. D. S. Heeschen and C. M. Wade (Dordrecht: Reidel), p. 211.
Riley, J. M. and Pooley, G. G. 1975, *Mem. R.A.S.*, **80**, 105.
Robson, D. W. 1981, *Nature*, **294**, 59.
Rudnick, L. 1982, in *IAU Syposium 97, Extragalactic Radio Sources*, ed. D. S. Heeschen and C. M. Wade (Dordrecht: Reidel), p. 47.
Rudnick, L., and Burns, J. O. 1981, *Ap. J. (Letters)*, **246**, L69.
Rudnick, L., Edgar, B. K., and Icke, V. 1984, in preparation.
Rudnick, L., Saslaw, W. C., Crane, P. C., and Tyson, J. A. 1981, *Ap. J.*, **246**, 647.
Ryle, M., and Longair, M. S. 1967, *M.N.R.A.S.*, **136**, 123.

Saikia, D. J. 1981, *M.N.R.A.S.*, **197**, 11P.
Saikia, D. J., and Wiita, P. J. 1982, *M.N.R.A.S.*, **200**, 83.
Sanders, R. H. 1983, preprint.
Saslaw, W. C., Valtonen, M. J., and Aarseth, S. J. 1974, *Ap. J.*, **190**, 253.
Saunders, R., Baldwin, J. E., Pooley, G. G., and Warner, P. J. 1981, *M.N.R.A.S.*, **197**, 287.
Scheuer, P. A. G., and Readhead, A. C. S. 1979, *Nature*, **277**, 182.
Shklovsky, I. S. 1977, *Astr. Zh.*, **53**, 713.
———. 1982, in *IAU Symposium 97, Extragalactic Radio Sources*, ed. D. S. Heeschen and C. M. Wade (Dordrecht: Reidel), p. 475.
Strom, R. G., Baker, J. R., and Willis, A. G. 1981, *Astr. Ap.*, **100**, 220.
Valtonen, M. J. 1979, *Ap. J.*, **231**, 312.
van Bruegel, W. J. M., and Willis, A. G. 1981, *Astr. Ap.*, **96**, 332.
van Groningen, E., Miley, G. K., and Norman, C. 1980, *Astr. Ap.*, **90**, L7.
Wiita, P. J., and Siah, M. J. 1981, *Ap. J.*, **243**, 710.
Willis, A. G., and Strom, R. G. 1978, *Astr. Ap.*, **62**, 375.
Willis, A. G., Strom, R. G., Bridle, A. H., and Fomalont, E. B. 1981, *Astr. Ap.*, **95**, 250.
Willis, A. G., Wilson, A. S., and Strom, R. G. 1978, *Astr. Ap.*, **66**, L1.

B. K. EDGAR and L. RUDNICK: University of Minnesota, Department of Astronomy, School of Physics and Astronomy, 116 Church Street, S.E., Minneapolis, MN 55455